A Comparative Study of Photon Radiation-Shielding Properties of Different Glass Types for Use in Health Facilities

Judith Nyangoma and Bosco Oryema, Muni University

Abstract

The usage of X-ray generating devices and gamma-ray sources such as 60Co and 137Cs for medical diagnostic and therapeutic applications has increased globally. However, exposure to radiation from these sources can cause detrimental effects on biological tissues. Thus, to optimise radiation safety, effective radiation shields are required. This study used the photon shielding and dosimetry (PSD) software to simulate and compare the photon shielding properties of phosphate, bismuthate, tellurite, silicate and borate glass for use in medical facilities. The parameters investigated included mass attenuation coefficient (MAC), linear attenuation coefficient (LAC), half-value layer (HVL), mean-free path (MFP), and effective atomic number (Z_{eff}). The results showed that bismuthate glass had the highest MAC and LAC values followed by tellurite, silicate, phosphate and borate glass respectively. It was also found that bismuthate glass had the lowest HVL and MFP values followed by tellurite, silicate, phosphate and borate glass. Since materials with high MAC and LAC and low HVL and MFP are associated with higher photon stoppage powers, bismuthate glass are better photon shielding materials compared to the rest of the glass examined in this study. Conversely, borate glass presented the least shielding potential compared to phosphate, silicate and tellurite glass.

Keywords: Radiation attenuation coefficients, Phy-X/PSD software, radiation-shielding parameters, radiation effects, bismuthate glass shields, borate glass shields

Introduction

Humans occasionally encounter radiation in the field of medicine during radiology, cardiology and radiotherapy procedures (Ruengsri, 2014). However, excessive exposure to ionising radiation may result in temporal or permanent tissue damage, acute radiation syndrome, and enhanced cancer risks (Dowlath *et al.*, 2021). This can be even worse for radiation workers as they can get exposed to enhanced radiation levels or accumulate higher doses over time due to the nature of their jobs. One of the measures of radiation protection that must be put in place to safeguard radiation workers (staff) from excessive exposure to ionising radiation is the use of effective radiation shields. A radiation shield absorbs the incoming photons and reduces the radiation intensity to safe levels, thereby protecting humans. Radiation shields vary from metal sheets to concrete and glass (Mhareb *et al.*, 2020). Simple lead has historically been the most common photon radiation shield because of its high density, making it highly effective at attenuating photons. However, due to its toxic nature, there is restricted use of it in medical treatment facilities (El-Mallawany *et al.*, 2018). Therefore, environmentally friendly substitutes for lead that are just as effective have been studied by many researchers to reduce lead toxicity. Concrete is a great candidate for this because of its low cost, simple manufacturing, and wide range of composition (Saddeek *et al.*, 2020). However, concrete is prone to cracking and water loss over time. This has led researchers to seek alternative materials.

Radiation-shielding glass come with the additional advantage of being transparent and not cracking, as well as providing the same benefits as concrete (Yasmin *et al.*, 2018). Transparency is important for viewing activities in the adjacent room while carrying out radiological procedures and is also applied in non-medical situations (Almatari *et al.*, 2019). Radiology uses average energies of 20 keV (dental), 30 keV (mammography), 40 keV (general) and 60 keV (computed tomography), respectively. Since these energies are the typical energy levels of photons used in the medical field, the glass investigated in this study were examined under these energy ranges (Abouhaswa *et al.*, 2021). The Phy-X/PSD software was used to determine the radiation-shielding properties such as mass attenuation coefficient (MAC), linear attenuation coefficient (LAC), half-value layer (HVL), effective atomic number (Z_{eff}), and the mean-free path (MFP) of the borate, tellurite, silicate, phosphate and bismuthate glass. These parameters are basic quantities often used for analysing the penetration and the energy deposition by photons. It is worth noting that the quality of data produced by modern simulation codes is limited to the quality of the embedded data libraries. The MAC describes the fraction or amount of incident photons absorbed in a unit mass of an absorber material. MAC is a useful parameter for finding the radiation leaving the materials.

On the other hand, LAC describes the attenuation of radiation per unit length of a material. In simple terms, LAC is the probability of interaction between radiation and the material per distance (Sayyed *et al.*, 2021). It characterises how easily a photon beam can penetrate a material volume. HVL is the thickness of a material required to reduce the intensity of a photon beam to half of its original value. The HVL values directly depend on the composition, density and structural arrangements of the constituents of a material. It is merely a proxy measure of the penetrating power of a photon beam, also known as beam quality (Waly *et al.*, 2018a). A lower HVL represents a better radiation-shielding property of a material. In photon shielding, these parameters are key in describing the ability of a photon beam to interact with and deposit its energy in the shielding material. The effective atomic number (Z_{eff}) represents the total number of electrons surrounding the nucleus of an atom. It comprises a metal atom's electrons and the bonding electrons from the surrounding electron-donating atoms and molecules, and it is closely related to the electron density, expressed in the number of electrons per unit mass (Manohara *et al.*, 2008). The MFP is the average distance radiation travels in a material before it undergoes another interaction.

Materials

The materials investigated in this study include phosphate, borate, silicate, bismuthate and tellurite glass. The glasses were coded as S1, S2, S3, S4 and S5, respectively as shown in Table 1. Table 1 also contains the chemical formulae, average molecular weight, densities of the glass under examination, and weight fractions of the constituent elements in these glass.

Table 1: Sample codes and their compositions

Code	Sample name	Chemical formula	AMW (g/mol)	Density (g/cm^3)	Weight fraction of elements (%)					
					O	P	B	Si	Bi	Te
S1	Phosphate glass	P_2O_5	141.94	2.39	0.5636	0.4364				
S2	Borate glass	B_2O_3	69.62	2.46	0.6894		0.3106			
S3	Silicate glass	SiO_2	60.08	2.65	0.5326			0.4674		
S4	Bismuthate glass	Bi_2O_3	465.96	8.9	0.1030				0.8970	
S5	Tellurite glass	TeO_4	191.60	6.24	0.3340					0.6660

Methods

Calculation of mass and linear attenuation coefficients

The MAC and LAC (μ) of the different glass types were determined using the Phy-X/PSD simulation software. The Phy-X software is an online simulation software that is used to calculate photon dosimetry and shielding properties of different shielding materials (Hussein *et al.*, 2022). The calculated values of the linear attenuation coefficient were used to determine the HVL and MFP as discussed below.

Calculation of half-value layer

In radiation protection through shielding, the goal is to reduce the intensity of the incident beam as much as possible, even with the smallest material thickness. So, finding a material that can reduce a beam intensity by half within a minimal material depth (i.e. a material with the lowest HVL) is of interest in radiation shielding. In this study, the HVL calculations for the different glass types were done using the equation (Al-Buriahi *et al.*, 2019):

$$\mathrm{HVL} = \frac{\ln 2}{\mu}$$

where μ is the LAC of the glass.

Calculation of effective atomic number

The effective atomic numbers of the different glass types were also determined using the Phy-X/PSD simulation software (Hussein *et al.*, 2022). In Atomic and Nuclear Physics, the atomic number Z (i.e. the number of protons in the nucleus) of an atom is a desired parameter in radiation-shielding design because it exhibits a strong and fundamental relationship with the nature of radiation interactions with that medium. However, for complex media such as compounds and other composite systems, a single atomic number cannot be used as the atomic number of a material composed of several elements. In this case, the effective atomic number, Z_{eff}, is a convenient parameter in radiation-shielding calculations so that the various atomic numbers in the material have to be weighted differently for the different photon interaction mechanisms with the matter (Manohara *et al.*, 2008).

Calculation of mean-free path

The MFP represents the statistically averaged distance a photon travels before it is absorbed or scattered in target materials. The MFP is an important parameter in radiation-shielding design when determining the thickness or depth of the material that can effectively stop a photon beam. When the thickness of the shielding material is much shorter than the photon's MFP, the photons propagate throughout the device practically without collision – this is the so-called ballistic transport regime (Dragoman and Dragoman, 1999). Mathematically, MFP is inversely proportional to LAC and is defined as (Singh *et al.*, 2018):

$$\mathrm{MFP} = \frac{1}{\mu}$$

Results and discussion

The mass attenuation coefficient

The values of MAC for all the samples under examination were computed with Phy-X/PSD software in the photon energy range between 15 and 15,000 keV. The variations of the MAC values versus the incident photon energies are shown in Figure 1. It can be seen from Figure 1 that MAC values changed with changes in primary photon energies. Here it can be observed that the MAC values generally decreased in the order of S4 > S5 > S1 > S3 > S2. Also, MAC values are seen to decrease with the increasing photon energy. This decrease in MAC values with increased photon energy is due to reduced dominance of photoelectric absorption in the high-energy region (Sayyed *et al.*, 2018). Since MAC is the measure of the fraction of incident photons absorbed per unit mass of a material, the photon energy, and thus photon interaction mechanisms, are crucial in determining the absorption cross-section. At low photon energies, the photoelectric effect is the most dominant interaction mechanism, while at higher energies, Compton scattering becomes predominant. At very high energies, pair production and photonuclear reactions become important. The overall effect is the observed decrease in attenuation with increased energy (Sayyed *et al.*, 2018). This explains why the MAC values of the investigated glass are highest in the low-energy region.

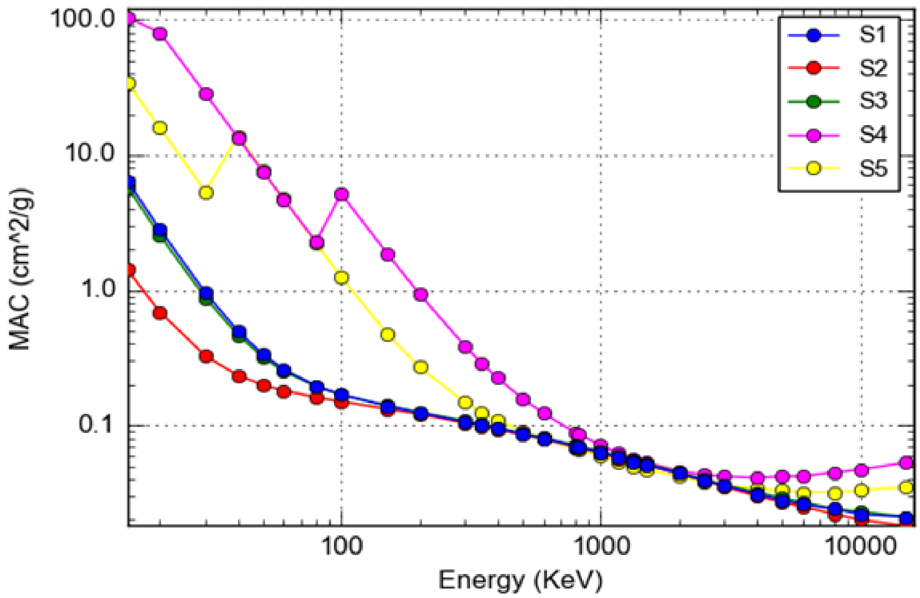

Figure 1: Variations of MAC values with incident photon energy

In the energy range of 15–50 keV, it was observed that the highest MAC values were in the S4 sample and the lowest MAC values were in the S2 sample. This shows that bismuthate glass have better absorption capacity than other comparative glass. It is also observed from **Figure 1** that there is a steep rise in the MAC values for S4 and S5 in the energy ranges of 80 to 100 keV and 20 to 50 keV respectively. This sudden increase is due to the K-shell absorption, which is a sudden increase in photon absorption occurring when the photon energy is just above the binding energy of the innermost electron shell of the atoms interacting with the photons (Bünyamin, 2020). S5 and S4 coincide together between 50 to 80 keV. Figure 1 also shows that the MAC values of all the glass samples coincide at 1500 keV. This is attributed to the Compton scattering effect, the most dominant photon interaction mechanism in this energy range. When high-energy photons interact with electrons of a target material, they transfer part of their kinetic energies to the orbital electrons and the photons change directions or frequencies. If the electrons attain sufficient energies beyond their binding energies, they are ejected from the atom, leaving the atoms ionised. MAC values of samples S4 and S5 slightly increased towards the maximum energy of 15,000 keV. This occurs in the high-energy range where pair production is dominant.

The linear attenuation coefficient

The energy-dependent variations of the LAC values are presented in Figure 2. Since the LAC values are obtained by multiplying the MAC values by density, the denser the material, the greater its LAC or the capacity to absorb radiation per unit of its length. Also, the higher the energy (wavelength) of the radiation, the greater its capacity to pass through a material. As seen in Figure 2, the variations of LAC values are similar to the changes in MAC values with changes in photon energy. It is also clearly seen in Figure 2 that all the samples have a continuous decrease in the LAC values with increasing photon energy. LAC values decreased in the order S4 > S5 > S1 > S3 > S2. It can also be seen that at 50 and 80 keV, S5 and S4 samples respectively indicated sharp jumps in their LAC values. S1 and S3 samples had their LAC values coincide from 0 to 60 keV. S1 and S2 samples had their LAC values coincide at photon energies between 120 and 1800 keV. S4 and S5 samples had higher LAC values, while S1 and S3 samples had average LAC values and the S2 sample had the least.

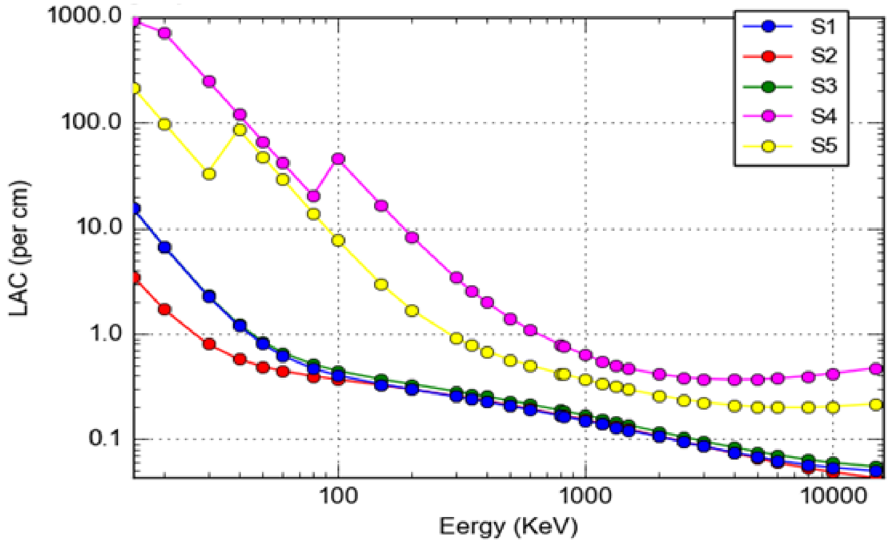

Figure 2: Variation of LAC values with energy

Half-value layer

The HVL is a common parameter used in radiation-shielding studies. Since HVL is inversely proportional to LAC, the higher the LAC value for a material, the lower its HVL and the better its radiation-shielding property. Figure 3 shows the variations in HVL values plotted against the photon energy. As seen from Figure 3, for all the samples investigated, the values of HVL increased with increasing photon energy in the order S4 < S5 < S3 < S1 < S2. This increase is due to the reduced photon interaction cross-section with atoms at high energies. Thus, the glass is more space-efficient at lower energies but is less space-efficient at higher energies.

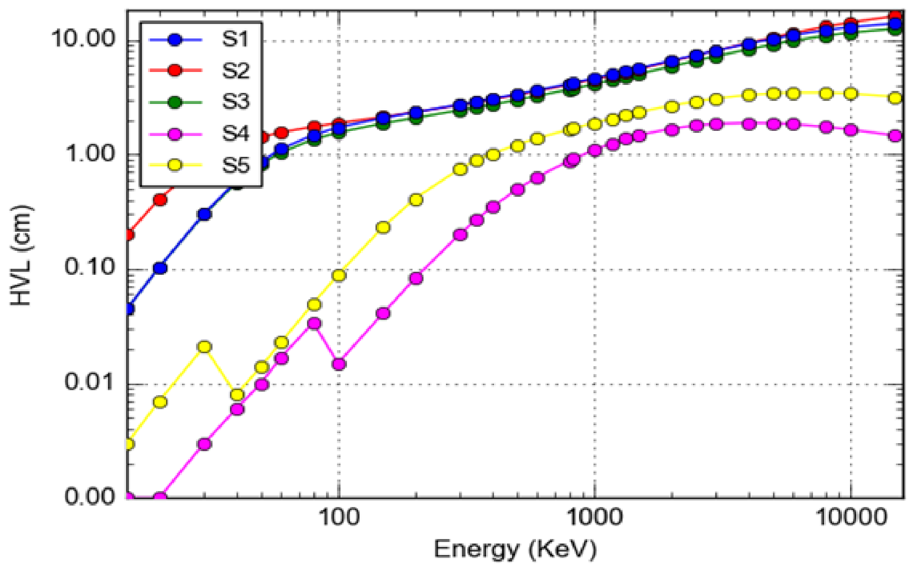

Figure 3: Variations of HVL values with energy

Mean-free path

Another important parameter investigated in this study is the MFP of photons in the different glass types. Similarly, MFP is inversely proportional to LAC. This implies that the higher the LAC values of a material, the lower its MFP and the better its radiation-shielding property. The physical meaning is that a material with higher LAC does not permit radiation to travel that deeply into the material. This is a crucial parameter to consider in radiation-shielding and design. The variations in MFP as a function of the incident photon energy for all the glass samples investigated in this study are presented in Figure 4. Figure 4 shows that MFP values increased with increasing photon energy. In the low-energy zone, these values are close to zero. However, in the region where Compton scattering dominates, photons tend to scatter and are less likely to be absorbed within the shielding material. Thus, thicker materials are needed since photons have longer mean-free paths (Waly *et al.*, 2018b). The scattered photons could travel in unpredictable/unexpected directions – for example, coming into contact with people. This is a problem that any shielding material must try to address to minimise human exposure to scattered photons. The sudden increase in HVL and MFP values in the middle energy region is attributed to the Compton scattering. By observing the variations in MAC, LAC, HVL and MFP values, it can be seen that the S4 sample has the best shielding characteristics among the examined samples.

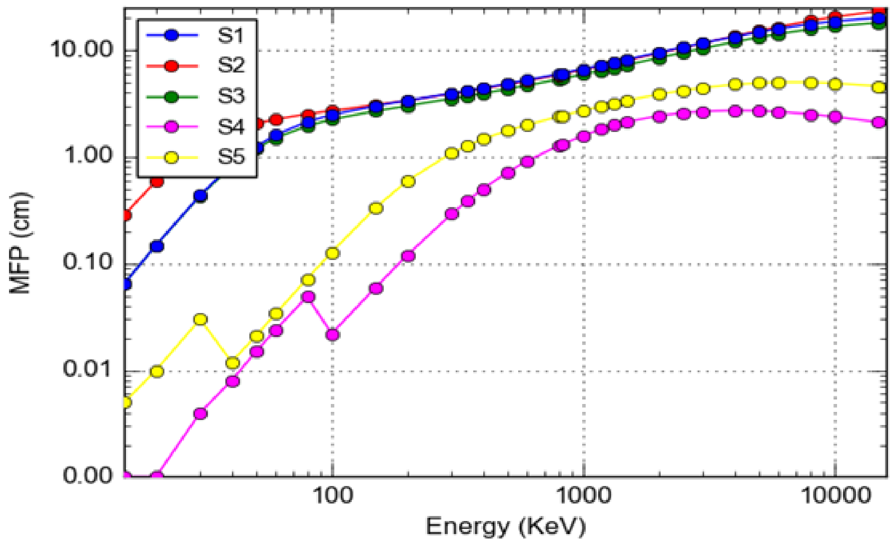

Figure 4: Variations of MFP values with incident photon energy

The effective atomic number

A single number for all energies cannot represent the atomic numbers of chemical compounds or mixtures as in the elements. So the effective atomic number, Z_{eff}, is used for composite samples. The variations in the effective atomic numbers with changes in incident photon energy are presented in Figure 5. The observed variations are in the order of S4 > S5 > S1 > S2. These variations are attributed to the photoelectric effect and coherent and incoherent scattering photon interaction mechanisms. Figure 5 shows that samples S1, S3 and S2 have low effective atomic numbers in the low-energy region, which remains almost constant in the high-energy region – except for S1 and S3, which slightly increase. It can also be seen that samples S4 and S5 have high values in the low-energy region which gradually decrease and rise again in the high-energy region. At the low-energy region, where the photoelectric effect is dominant, the incident photon interacts with the electrons in the material, and the photon loses its kinetic energy to either excite the electrons or dislodge them from their positions, causing ionisation of the atoms. As the photon energy increases, Compton scattering becomes predominant. In this case, the photon interacts with the electrons but the photon does not get stopped completely. Instead, they change directions and get scattered in the material while continuing to interact with the electrons, leaving behind trails of excited and dislodged electrons in the material. At higher photon energy, pair production becomes more predominant than in all the previous processes. In general conditions, effective atomic number values should be high in low-energy regions. This implies that S4 and S5 samples with high effective atomic number values in the low-energy region have better photon shielding properties than S1, S2 and S3 samples.

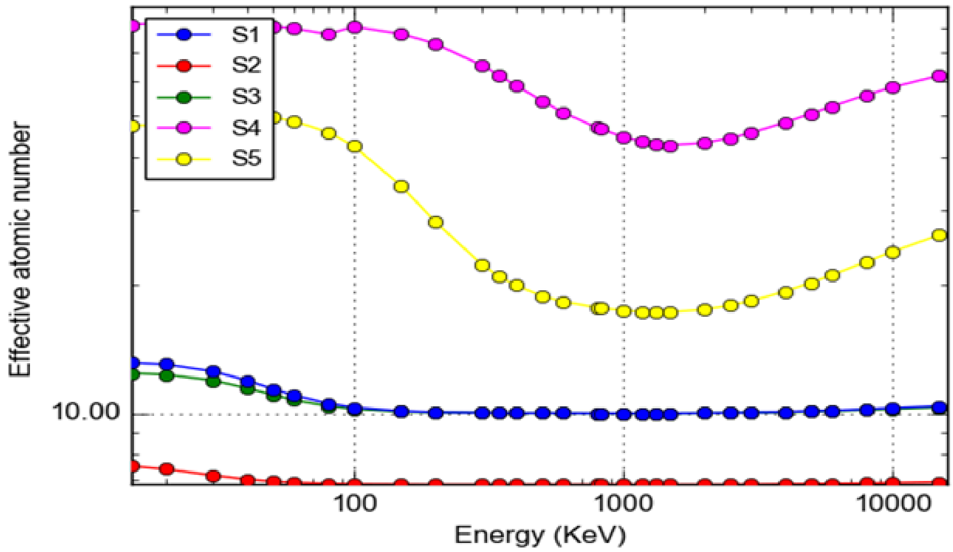

Figure 5: Variations of effective atomic number against energy

Conclusion

A study of the radiation-shielding properties of tellurite, bismuthate, silicate, borate, and phosphate glass was conducted using the Phy-X/PSD simulation software. The results showed that bismuthate glass (S4) had the highest MAC and LAC values followed by tellurite (S5), silicate (S3), phosphate (S1) and borate (S2) glass respectively. The results also showed that bismuthate glass had the lowest HVL and MFP values followed by tellurite, silicate, phosphate and borate glass respectively. Since materials with high MAC and LAC values, and low HVL and MFP values are better photon attenuators , this study found bismuthate glass to be better radiation-shielding material than the rest of the glass examined in this study. It is been observed that bismuthate glass has a higher density compared to other studied glass, which implies that density affects the shielding properties of a material. On the other hand, borate glass presented the least shielding potential compared to phosphate, silicate and tellurite glass. Borate glass was observed to have the least or lowest properties in shielding, making them the material with the worst shielding properties. It was observed that the weighting mole fractions of a compound affects its effective atomic number and its variations with photon energy; this was discovered when individual elements were studied with incident photon energy.

List of figures

List of tables

References

Abouhaswa, A. S., H. M. H. Zakaly, S. A. M. Issa, M. Rashad, M. Pyshkina, H. O. Tekin, R. El-Mallawany and M. Y. A. Mostafa, (2021). 'Synthesis, physical, optical, mechanical, and radiation attenuation properties of TiO2–Na2O–Bi2O3–B2O3 glasses', *Ceramics International*, *47* (1). https://doi.org/10.1016/j.ceramint.2020.08.122

Al-Buriahi, M. S., H. Arslan and B. T. Tonguc (2019). 'Mass attenuation coefficients, water and tissue equivalence properties of some tissues by Geant4, XCOM and experimental data', *Indian Journal of Pure and Applied Physics*, *57* (6), 433–37.

Almatari, M., O. Agar, E. E. Altunsoy, O. Kilicoglu, M. I. Sayyed and H. O. Tekin (2019). 'Photon and neutron shielding characteristics of samarium doped lead alumino borate glasses containing barium, lithium and zinc oxides determined at medical diagnostic energies', *Results in Physics*, *12*. https://doi.org/10.1016/j.rinp.2019.01.094

Bünyamin A. (2020). 'Determination of radiation protection features of the Ag2O doped boro-tellurite glasses using Phy-X / PSD software', *Journal of the Institute of Science and Technology*, *10* (1), 202–213. https://doi.org/10.21597/jist.640027

Dowlath, M. J. H., S. K. Karuppannan, P. Sinha, N. S. Dowlath, K. D. Arunachalam, B. Ravindran, S. W. Chang, P. Nguyen-Tri and D. D. Nguyen (2021). 'Effects of radiation and role of plants in radioprotection: A critical review', *Science of the Total Environment*, *779*. https://doi.org/10.1016/j.scitotenv.2021.146431

Dragoman, D and M. Dragoman (1999). 'Optical analogue structures to mesoscopic devices', *Progress in Quantum Electronics*, *23*, 131–88.

El-Mallawany, R., M. I. Sayyed, M. G. Dong and Y. S. Rammah (2018). 'Simulation of radiation shielding properties of glasses contain PbO', *Radiation Physics and Chemistry*, *151*, 239–52. https://doi.org/10.1016/j.radphyschem.2018.06.035

Hussein, K. I., M. S.Alqahtani, K. J.Alzahrani, F. F.Alqahtani, H. Y.Zahran, A. M.Alshehri, I. S.Yahia, M.Reben, and E. S. Yousef (2022), 'The effect of ZnO, MgO, TiO2, and Na2O modifiers on the physical, optical, and radiation shielding properties of a TeTaNb glass system', *Materials*, *15* (5). https://doi.org/10.3390/ma15051844

Manohara, S. R., S. M. Hanagodimath, K. S. Thind, L. Gerward (2008). 'On the effective atomic number and electron density: A comprehensive set of formulas for all types of materials and energies above 1 keV', *Nuclear Instruments and Methods in Physics Research B*, 266, 3906–12.

Mhareb, M. H. A., Y. S. M. Alajerami, M. I. Sayyed, N. Dwaikat, M. Alqahtani, F. Alshahri, N. Saleh, N. Alonizan, T. Ghrib and S. I. Al-Dhafar (2020). 'Radiation shielding, structural, physical, and optical properties for a series of borosilicate glass', *Journal of Non-Crystalline Solids*, *550*. https://doi.org/10.1016/j.jnoncrysol.2020.120360

Ruengsri, S. (2014). 'Radiation shielding properties comparison of Pb-based silicate, borate, and phosphate glass matrices', *Science and Technology of Nuclear Installations*, https://doi.org/10.1155/2014/218041

Saddeek, Y. B., S. A. M. Issa, T. Alharbi, R. Elsaman, G. Abd elfadeel, A. M. A. Mostafa, K. Aly and M. Ahmad (2020). Synthesis and characterization of lead borate glasses comprising cement kiln dust and Bi2O3 for radiation shielding protection. *Materials Chemistry and Physics*, *242*. https://doi.org/10.1016/j.matchemphys.2019.122510

Sayyed, M. I., B. Albarzan, A. H. Almuqrin, A. M. El-khatib, A. Kumar, D. I. Tishkevich, A. V, Trukhanov, and M. Elsafi (2021). 'Experimental and theoretical study of radiation shielding features of cao-k2o-na2o-p2o5 glass systems', *Materials (Basel) 14* (14):3772

Sayyed, M. I., M. G., Dong, H. O, Tekin, G, Lakshminarayana and M. A. Mahdi (2018). 'Comparative investigations of gamma and neutron radiation shielding parameters for different borate and tellurite glass systems using WinXCom program and MCNPX code', *Materials Chemistry and Physics*, *215*. https://doi.org/10.1016/j.matchemphys.2018.04.106

Singh, V. P., T. Korkut and N. M. Badiger (2018). 'Comparison of mass attenuation coefficients of concretes using FLUKA, XCOM and experiment results', *Radioprotection*, *53* (2), 145–148. https://doi.org/10.1051/radiopro/2018008

Waly, E. A., G. S. Al-qous and M. A. Bourham (2018a). 'Shielding properties of glasses with different heavy elements additives for radiation shielding in the energy range 15–300 keV', *Radiation Physics and Chemistry*, https://doi.org/10.1016/j.radphyschem.2018.04.029

Waly, E. A., Al-qous, G. S., and Bourham, M. A. (2018b). Author ' s Accepted Manuscript. *Radiation Physics and Chemistry*. https://doi.org/10.1016/j.radphyschem.2018.04.029

Yasmin, S., Barua, B. S., Khandaker, M. U., Chowdhury, F. U. Z., Rashid, M. A., Bradley, D. A., Olatunji, M. A., and Kamal, M. (2018). Studies of ionizing radiation shielding effectiveness of silica-based commercial glasses used in Bangladeshi dwellings. *Results in Physics*, *9*. https://doi.org/10.1016/j.rinp.2018.02.075

Glossary

Compton scattering: the process by which high-energy photons are scattered following their interactions with the electrons of a material

Gamma ray: a penetrating form of electromagnetic radiation that emanates from the radioactive decay of atomic nuclei.

Ionising radiation: radiation that carries sufficient energy to knock off electrons from the atoms or molecules of a material

keV: written in full as kilo electron volt, is the kinetic energy gained by a single electron accelerating through an electric potential difference of one volt in a vacuum.

Pair production: the process by which a high-energy photon creates an electron and a positron pair when it passes close to the nucleus of an atom

Photoelectric effect: the emission of electrons from a material following absorption of electromagnetic radiation such as gamma rays, X-rays and ultraviolet light.

Photon attenuator: a material with a high potential to stop photon radiation such as gamma rays and X-rays

Photon radiation: is a class of massless and chargeless particles or waves that form the electromagnetic spectrum.

Photon shielding: is the use of appropriate materials that can reduce the number of incoming photons and their energy to protect humans and the environment from their detrimental effects

Radiation attenuation: the process by which a material slows down or reduces the energy of an incoming radiation

Radiation dosimetry: is the measurement, calculation and assessment of the ionising radiation dose absorbed by an object, usually the human body.

Radiation syndrome: is a collection of health effects caused by exposure to high amounts of ionising radiation.

Radiation: is the emission or transmission of energy in the form of waves or particles through space or a material medium.

Radiology: is a branch of medicine that uses medical imaging to diagnose diseases and guide their treatment.

Radiotherapy: is the treatment of cancer using ionising radiation.

To cite this paper please use the following details: Nyangoma, J. and Oryema, B. (2024), 'A Comparative Study of Photon Radiation-Shielding Properties of Different Glass Types for Use in Health Facilities' *Reinvention: an International Journal of Undergraduate Research*, Volume 17, Issue S1, https://reinventionjournal.org/article/view/1376. Date accessed [insert date]. If you cite this article or use it in any teaching or other related activities please let us know by e-mailing us at Reinventionjournal@warwick.ac.uk.

https://doi.org/10.31273/reinvention.v17iS1.1376, ISSN 1755-7429, c 2024, contact, reinventionjournal@warwick.ac.uk